catalysts

MDPI

Article

Enzyme-Catalyzed Glycosylation of Curcumin and Its Analogues by Glycosyltransferases from *Bacillus subtilis* ATCC 6633

Yatian Cheng [1,†], Jian Zhang [2,†], Yan Shao [2], Yixiang Xu [2], Haixia Ge [3], Boyang Yu [1] and Weiwei Wang [1,*]

1 Jiangsu Key Laboratory of TCM Evaluation and Translational Research, School of Traditional Chinese Pharmacy, China Pharmaceutical University, Nanjing 211198, China
2 State Key Laboratory of Natural Medicines, China Pharmaceutical University, Nanjing 210009, China
3 School of Life Sciences, Huzhou University, Huzhou 313000, China
* Correspondence: weiweiwang@cpu.edu.cn; Tel.: +86-25-8618-5157; Fax: +86-25-8618-5158
† Contributed equally to this work.

Received: 18 July 2019; Accepted: 26 August 2019; Published: 29 August 2019

Abstract: Curcumin is a naturally occurring polyphenolic compound that is commonly used in both medicine and food additives, but its low aqueous solubility and poor bioavailability hinder further clinical applications. For assessing the effect of the glycosylation of curcumin on its aqueous solubility, two glycosyltransferase genes (*BsGT1* and *BsGT2*) were cloned from the genome of the strain *Bacillus subtilis* ATCC 6633 and over-expressed in *Escherichia coli*. Then, the two glycosyltransferases were purified, and their glycosylation capacity toward curcumin and its two analogues was verified. The results showed that both *BsGT1* and *BsGT2* could convert curcumin and its two analogues into their glucosidic derivatives. Then, the structures of the derivatives were characterized as curcumin 4′-O-β-D-glucoside and two new curcumin analogue monoglucosides namely, curcumoid-O-α-D-glucoside (**2a**) and 3-pentadienone-O-α-D-glucoside (**3a**) by nuclear magnetic resonance (NMR) spectroscopy. Subsequently, the dissolvability of curcumin 4′-O-β-D-glucoside was measured to be 18.78 mg/L, while its aglycone could not be determined. Furthermore, the optimal catalyzing conditions and kinetic parameters of *BsGT1* and *BsGT2* toward curcumin were determined, which showed that the Kcat value of *BsGT1* was about 2.6-fold higher than that of *BsGT2*, indicating that curcumin is more favored for *BsGT2*. Our findings effectively apply the enzymatic approach to obtain glucoside derivatives with enhanced solubility.

Keywords: curcumin 4′-O-β-D-glucoside; glycosyltransferases; *Bacillus subtilis* ATCC 6633

1. Introduction

Curcumin (diferuloylmethane) is extracted from the rhizome of traditional Chinese medicine *Zedoary turmeric* and *Curcuma longa*, and is a natural polyphenolic compound that is used as a food coloring in pastries, mustards, curries, and dairy food, as well as rice, meat, and fish dishes in the USA and England [1,2]. Besides these usages, curcumin exerts promising pharmacological properties, such as anti-oxidant, anticancer, anti-inflammatory and antifibrinolytic effects [3–5]. Thus, it has long been believed to be a potential protective natural compound against cardiac diseases, and to possess hepatoprotective and nephroprotective activities [6]. Over the past several decades, extensive research has demonstrated its possible action mechanisms, such as inhibiting experimental allergic encephalomyelitis in the treatment of multicentric sclerosis [7], and as a sarcoplasmic/endoplasmic reticulum calcium pump against cystic fibrosis [8]. However, a few drawbacks of curcumin, including poor pharmacokinetic/pharmacodynamic (PK/PD) properties, low aqueous solubility, and poor

bioavailability have hindered its further clinical applications [9–11]. While many curcumin analogues have been synthesized in an attempt to unearth new substitutes, none have possessed good drug candidate properties [12]. Thus, this is an imperative issue that has attracted scientists' interest in significantly improving its aqueous solubility.

The glycosylation of natural products (NPs) has the potential to enhance the aqueous solubility of hydrophobic compounds notably, and catalysis by GTs (glycosyltransferases) plays a prominent role in drug discovery and development [13–15]. GTs (EC 2.4.x.y) comprise a great family of enzymes that get involved in the biosynthetic pathways of saccharides and glycoconjugates [16]. Among these, uridine diphosphate-glycosyltransferases (UGTs) can transfer a sugar residue to particular acceptor compounds from an activated nucleotide sugar donor, (for example, uridine diphosphate (UDP)-sugars), forming glycosidic bonds. Currently, the enzymatic synthesis of NP glucosides is more ecofriendly and less time-consuming with higher final-product yields in contrast to chemical synthesis approaches. Therefore, the strategy of enzymatic synthesis of NP glucosides by GTs has been to develop a means to obtain glycosylated small molecules. For example, *Bs-YjiC* (a GT from *Bacillus subtilis* 168) could transfer a glucosyl moiety to three particular free OHs of protopanaxatriol, forming its glucoside derivatives [17], and a UGT from *Bacillus licheniformis* was elucidated for the glycosylation of phloretin to produce five phloretin glucosides [18]. Moreover, it is encouraging that a fungal GT from *Mucor hiemalis* exerts the substrate promiscuity of the 72 structurally diverse drug-like natural products [19].

Our previous studies have discovered that *Bacillus subtilis* ATCC 6633 showed excellent glycosylation capacity toward a few natural products [20]. In this research, we found that the strain *B. subtilis* ATCC 6633 could convert curcumin to its glucoside derivative. To identify the enzymatic system involved in the glycosylation, two GT genes (*BsGT1* and *BsGT2*) were cloned from *B. subtilis* ATCC 6633 and over-expressed in *Escherichia coli* (*E. coli*). Phylogenetic analysis and sequence alignment with several representative GTs were also investigated. Later, we identified two GTs' glycosylation activity toward curcumin and its two analogues. Then, preparative-scale reactions were conducted, and the glycosylated products of curcumin and its two analogues were isolated and their structures were elucidated. After this, the optimal catalyzing conditions and kinetic parameters of *BsGT1* and *BsGT2* toward curcumin were determined. Then, the aqueous solubility of the curcumin and its glucoside derivative were measured.

2. Result

2.1. Biotransformation of Curcumin with B. Subtilis ATCC 6633

Our previous research discovered that *B. subtilis* ATCC 6633 could convert the pentacyclic triterpenes to their glucoside derivatives [20]. To confirm whether this strain could also transform curcumin, it was cultivated in broth with curcumin, and then, the fermentation liquor was analyzed by high-performance liquid chromatography (HPLC).

Figure 1 shows the HPLC analysis of the 16-h fermentation broth of the strain *B. subtilis* ATCC 6633 fed with curcumin. In Figure 1, curcumin appears at the retention time (RT) of 29.3 min. After 16 h of fermentation, a new peak with a RT of 19.3 min appeared. To verify whether the metabolite is the glucoside derivative of curcumin, liquid chromatography-mass spectrometry (LC-MS) analysis was implemented. The results showed that the molecular ion peak of the new peak of the fermentation broth in the presence of curcumin added 162 Da compared with curcumin (shown in Supplementary Materials Figure S1). Consequently, it was concluded that curcumin was transformed by *B. subtilis* ATCC 6633.

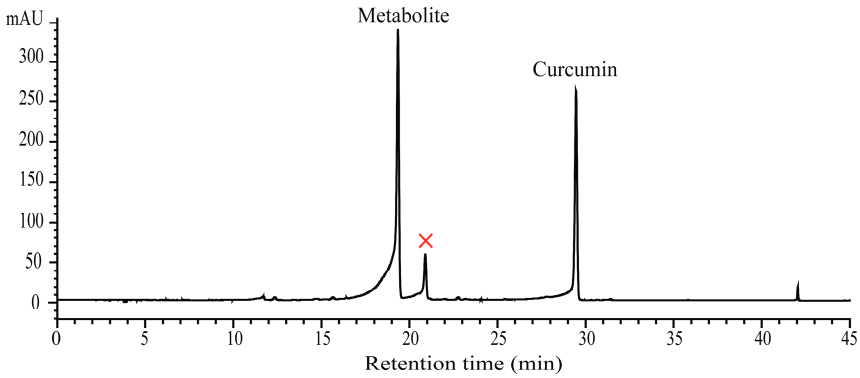

Figure 1. Biotransformation of curcumin by *B. subtilis* ATCC 6633. The strain was cultivated in potato dextrose culture medium containing curcumin 1.0 mg/50 mL. The 16-h cultivations of the fermentation broth were extracted with 50 mL of ethyl acetate three times, and the organic phase was concentrated and dissolved in methanol for HPLC analysis.

2.2. Purification of Recombinant BsGT1 and BsGT2

The recombinant *BsGT1* and *BsGT2* with His-tags were expressed heterologously in *E. coli* BL21 and purified through a His-tag Ni-NTA (nitrilotriacetic acid) affinity column. SDS-PAGE analysis indicated that the two purified proteins both showed a molecular mass above the 43-kDa protein marker, which was in good keeping with the sum of the predicted molecular weights of 44.0 kDa for *BsGT1* and 44.5 kDa for *BsGT2* (Figure 2). The concentration of purified protein was tested by the BCA kit method (Thermo Scientific, China).

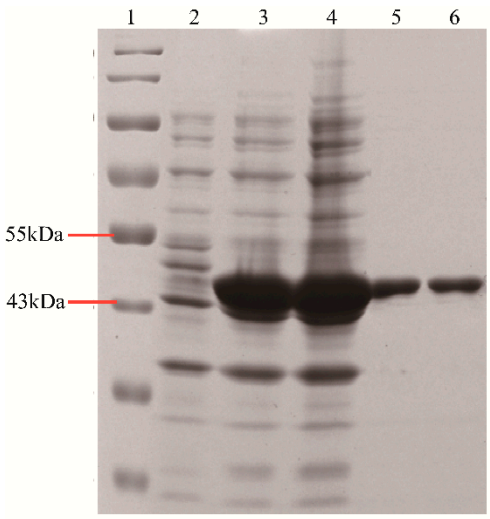

Figure 2. Expression and purification of the recombinant *BsGT1* and *BsGT2*. 1, protein marker; 2, the lysate of *E. coli* with empty plasmid pET-28a (+); 3, soluble protein of recombinant *BsGT1* after induction; 4, soluble protein of recombinant *BsGT2* after induction; 5, purified recombinant *BsGT1*; and, 6, purified recombinant *BsGT2*.

2.3. Detection of Glycosylated Products by HPLC-QTOF-MS

For determining the glycosylation activity of *BsGT1* and *BsGT2* toward curcumin and its two analogues, the reactions were conducted with 5 μg of two purified proteins in 300 μL of reaction buffer (50 mM of Tris-HCl pH 8.0) which contained 1.37 mM of UDP-glucose (UDP-Glc) and 2-μL substrates (10 mg dissolved in 500 μL of DMSO, respectively), and maintained at 37 °C for 3 h. Then, an extract of each reaction was analyzed by HPLC. All the reactions displayed a new peak at an earlier RT when compared with the substrates (shown in Figures S2 and S3). HPLC-QTOF-MS

was conducted to further elucidate whether 162 Da was added to different phenolic hydroxyl groups when compared with that of each substrate. As shown in Figure 3, 162 Da was added to Compounds **1a** ([M-H]$^-$, m/z = ~529.17), **2a** ([M-H]$^-$, m/z = ~527.23), and **3a** ([M-H]$^-$, m/z = ~487.19) corresponding to the molecular formulae $C_{27}H_{30}O_{11}$, $C_{28}H_{32}O_{10}$, and $C_{25}H_{28}O_{10}$, respectively, and these were preliminarily identified as monoglucosides of substrates **1**~**3**.

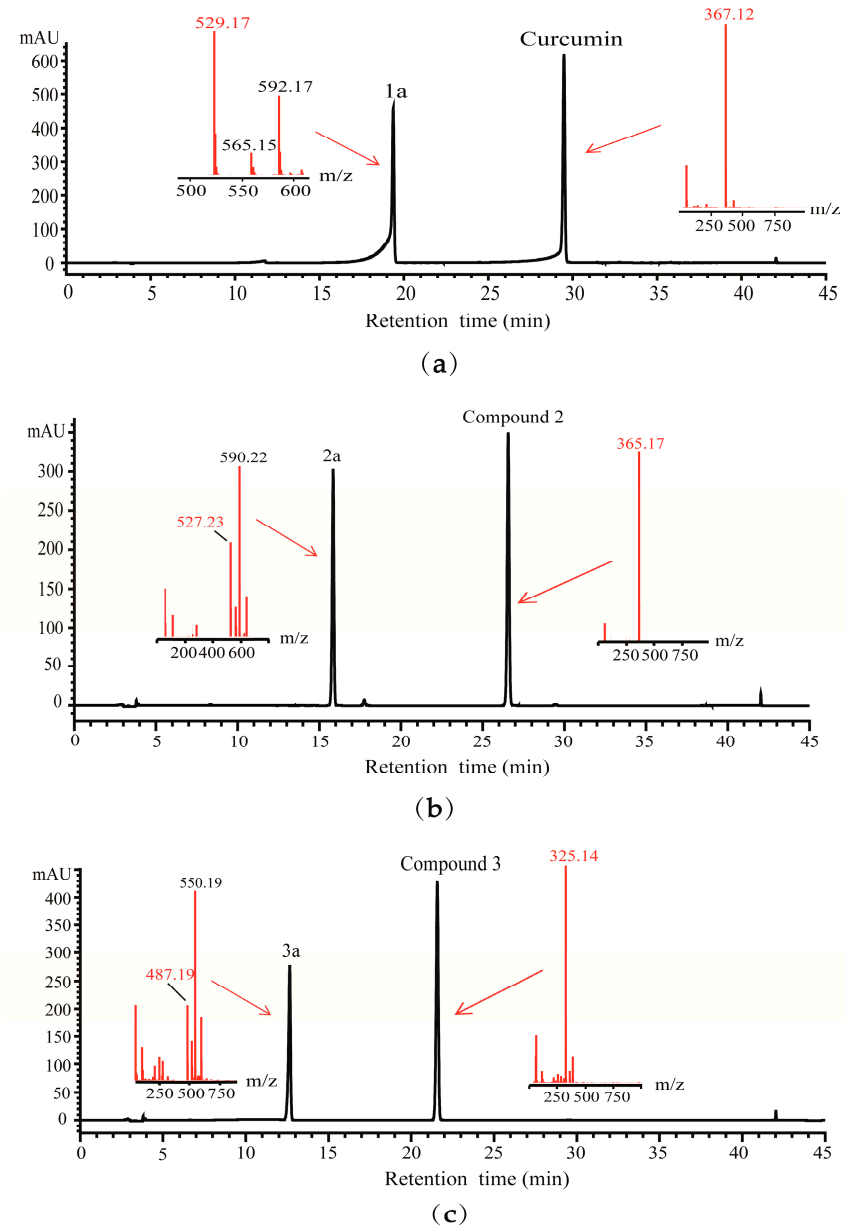

Figure 3. HPLC analysis of the glucoside derivatives of curcumin **1** (**a**) and its analogues **2** (**b**) and **3** (**c**) catalyzed by *BsGT1*, and QTOF-MS analysis of those catalyzed by *BsGT1* and *BsGT2* (red numbers are molecular ion peaks [M-H]$^-$ of glucoside derivatives and substrates).

2.4. Structural Elucidation of Curcumin and Its Two Analogues Glucoside Derivatives

For further elucidation of the structures of these Compounds **1a**, **2a**, and **3a,** the purified products were subjected to ^{1}H NMR and ^{13}C NMR analysis, as described in the Supporting Materials (Figures S4–S6). In addition to the signals of the curcumin, and Compounds **1** and **2** moieties, six carbon signals (from 62.98 to 102.15 ppm of **1a**, from 60.78 to 99.95 ppm of **2a**, and from 61.22 to 100.12 ppm of **3a**) belonging to the structure of the glucose moiety were examined. As shown in

the ^{1}H NMR spectra, the anomeric proton signals at δ 5.04 (J = 7.3 Hz), 5.26 (J = 4.1 Hz), and 5.26 (J = 4.8 Hz) of Compounds **1a**, **2a**, and **3a**, respectively indicated the β-configuration of Compound **1a** and the α-configuration of Compounds **2a** and **3a** for the glucopyranosyl moiety. The ^{13}C NMR spectra showed the glucose anomeric carbon at δ 102.15, 99.95, and 100.12 (glycosidation shift), respectively. In addition, the ^{1}H NMR and ^{13}C NMR analysis certified that the structure of Compound **1a** was curcumin 4′-O-β-D-glucoside, and the structures of Compounds **2a** and **3a** were O-α-D-glucosides. The illustration of the enzyme-catalyzed glycosylation of curcumin, and Compounds **2** and **3** by *BsGT1* and *BsGT2*, are shown in Scheme 1.

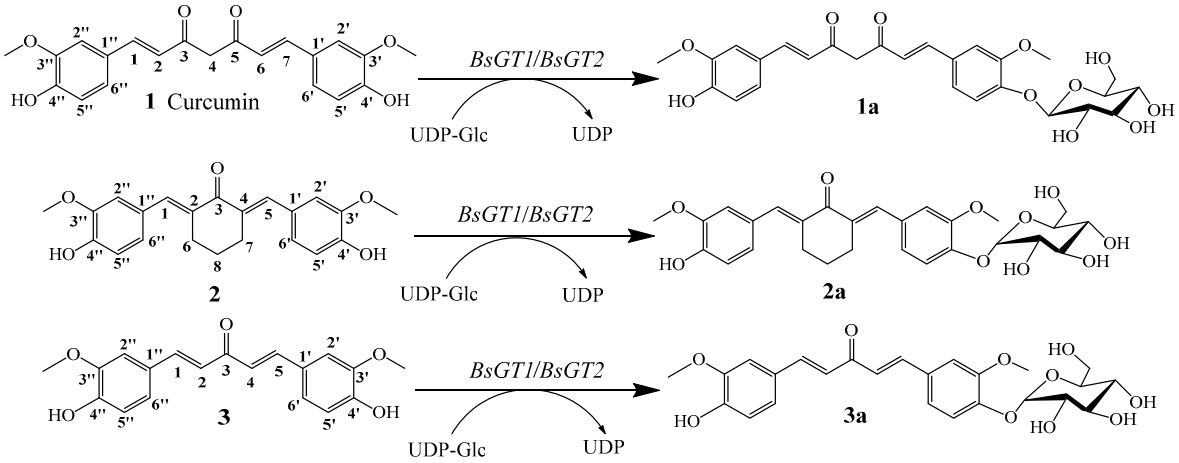

Scheme 1. Catalysis of curcumin and its two analogues by *BsGT1*/*BsGT2*. Compound **1a** is curcumin 4′-O-β-D-glucoside.

2.5. Optimal Catalyzing Conditions and Kinetic Parameters of BsGT1 and BsGT2 toward Curcumin

In order to determine the optimal catalytic condition by *BsGT1* and *BsGT2*, the influence of temperature, pH values, and metal ions on enzymatic activity was examined. As shown in Figure 4, both *BsGT1* and *BsGT2* showed optimal activity at pH 8.0. The optimum temperatures of *BsGT1* and *BsGT2* were both 40 °C. However, we found that the two GTs have lower catalytic efficiency at 50 °C. Moreover, they both favored $MnCl_2$ as their cofactor, which was in accordance with GTs using divalent metal ions as cofactors, such as Mn^{2+} and Mg^{2+}. As shown in the results, the optimal catalyzing conditions for both *BsGT1* and *BsGT2* are 40 °C and pH 8.0 with 20 mM of Mn^{2+}.

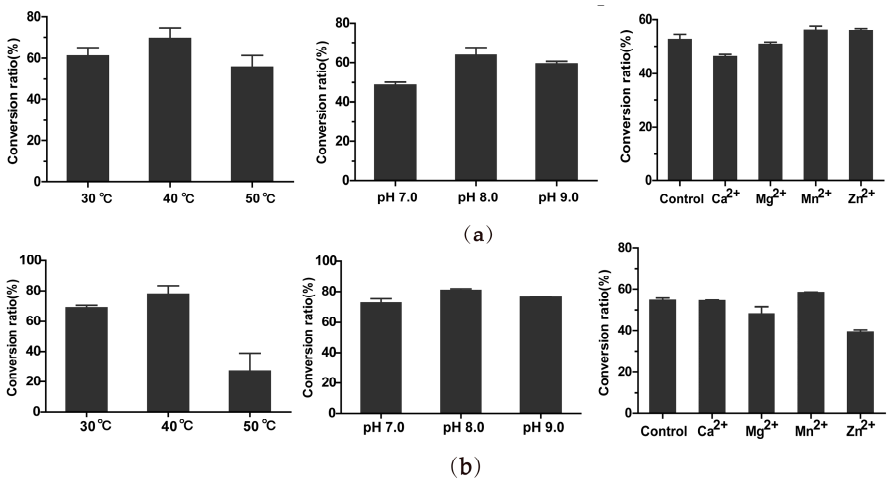

Figure 4. Effects of temperature, pH, and metal ions on *BsGT1* (**a**) and *BsGT2* (**b**) activity in the biosynthesis of curcumin monoglucoside. The mean (n = 2) is shown, and the error bars represent standard deviations.

The kinetic parameters of purified *BsGT1* and *BsGT2* toward curcumin were determined as shown in Table 1. The Km values of *BsGT1* and *BsGT2* for curcumin are 200.1 ± 23.73 μM and 118.3 ± 17.69 μM, respectively, indicating that curcumin is more favored for *BsGT2* than *BsGT1*. The Kcat of *BsGT1* is about 2.6-fold higher than that of *BsGT2*.

Table 1. Kinetic parameters of *BsGT1* and *BsGT2* toward curcumin. GTs: glycosyltransferases.

GTs	Km (μM)	Kcat (S^{-1})	Vmax (μM·min^{-1})
BsGT1	200.1 ± 23.73	0.47 ± 0.03	45.31 ± 2.50
BsGT2	118.3 ± 17.69	0.18 ± 0.01	24.87 ± 1.37

2.6. Determination of Solubility of Curcumin and Curcumin 4′-O-β-D-glucoside

The aqueous solubility of curcumin and curcumin 4′-O-β-D-glucoside was examined, and is summarized in Table 2. It is generally accepted that curcumin has extremely poor solubility in water, but that one or more saccharide groups of conjuncted aglycone could improve its aglycone's aqueous solubility. The results revealed that curcumin possessed aqueous solubility after glycosylation.

Table 2. Aqueous solubility of curcumin and curcumin 4′-O-β-D-glucoside.

Compound	Aqueous Solubility (mg/L)
Curcumin	N.D [1]
Curcumin 4′-O-β-D-glucoside	18.78

[1] 'N.D' means 'Not detected'.

2.7. Phylogenetic Analysis and Sequence Alignment

Phylogenetic analysis of *BsGT1*, *BsGT2*, and 20 GTs from plants, bacteria, and fungi was constructed with MEGA 7.0, as shown in Figure 5. The phylogenetic tree divided those GTs into two parts (red numbers 1 and 2), and it is worth considering that the first part includes plant GTs and microbial GTs, which might indicate that *BsGT1* and *BsGT2* have a closer phylogenetic relationship with some plant UGTs than some microbe ones. To aid further understanding, several representative plant and microbial GTs were aligned based on amino acid sequences.

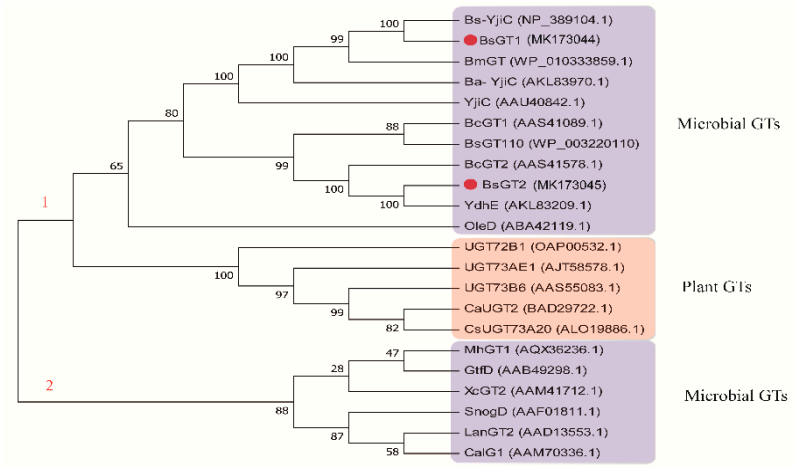

Figure 5. Phylogenetic analysis of *BsGT1*, *BsGT2*, and 20 GTs from plants, bacteria, and fungi. The tree, whose substitution model was Poisson correction, was constructed with the neighbor-joining method based on 1000 bootstrapping cycles. Black numbers at each branch point represent the bootstrap values in the form of percentage. The sequences' GenBank accession numbers are also given.

Sequence alignment, based on the full-length proteins of *BsGT1*, *BsGT2*, and eight selected functionally characterized GTs from plants and bacteria, demonstrated that those microbial GTs showed notably higher homology and similarity with the highly conserved plant secondary product glycosyltransferase (PSPG) motif in plant-derived family 1 GTs [21] (Figure 6). This could give insight into GTs' evolutionary relationship between plants and microbes. Moreover, *BsGT1* has a closer phylogenetic relationship with *Bs-YjiC*, which is a promiscuous GT from B. subtilis 168, showing that it may largely possess substrate flexibility and power regiospecificity.

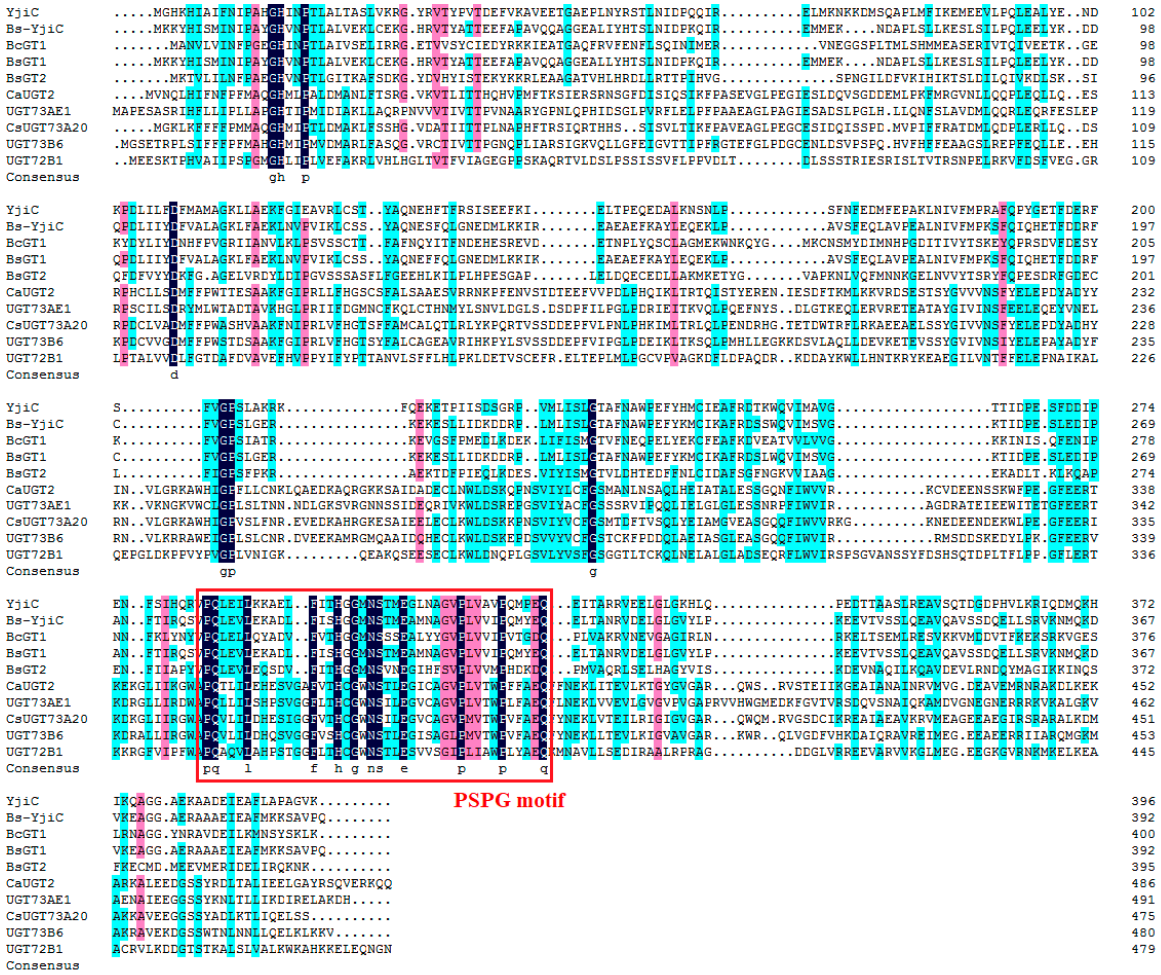

Figure 6. Sequence alignment based on the full-length proteins of *BsGT1*, *BsGT2*, and eight GTs from plants and bacteria, and the five GTs from plants are involved in the glycosylation of secondary metabolites. The PSPG box is marked by the red rounded rectangle.

3. Discussion

A number of biologically active compounds are glucosides, and even the glycosidic residue plays a central role in their activity; for example, it can improve aglycones' pharmacokinetic parameters and water solubility. Curcumin has been proven to possess multiple bioactivities, but a few drawbacks, including its poor PK/PD properties, low aqueous solubility, or poor bioavailability, hinder further applications. Here, two GTs from *B. subtilis* ATCC 6633 were cloned and over-expressed to biosynthesize curcumin 4′-O-β-D-glucoside. Then, an aqueous solubility test of curcumin and curcumin 4′-O-β-D-glucoside indicated that curcumin 4′-O-β-D-glucoside had more preferable aqueous solubility. The pharmacological properties of these biosynthesized glucosides should be further studied, and deep structural analysis of *BsGT1* and *BsGT2* should also be undertaken to elucidate the difference in catalytic properties. Furthermore, this method could be applied to boost the aqueous solubility

and bioavailability of other active hydrophobic compounds, and it would be of great interest to introduce the two GTs into glucoside-producing chassis cells to accelerate the production of natural or natural-like active glucosides via metabolic engineering [17].

4. Materials and Methods

4.1. Microorganisms, Plasmids, and Chemicals

B. subtilis ATCC 6633 was a kind present of Prof. J. P. N. Rosazza of the University of Iowa (Iowa, IA, USA). The two curcumin analogues [22] were synthesized by our laboratory, and could be used as analytical compounds. Curcumin and UDP-glucose (UDP-Glc) were purchased from Aladdin (Aladdin, Shanghai, China). pET-28a (+) was purchased from Novagen (Madison, WI, USA). Other biological reagents were obtained from Takara, except for the His-tag Ni-NTA affinity column, which was purchased from Beyotime (Beyotime, Shanghai, China). HPLC-grade acetonitrile was bought from Tedia Co., Ltd (Fairfield, OH, USA), and *E. coli* BL21 (DE3) (Transgen Biotech, Beijing, China) was cultivated in Luria Bertani (LB) medium, which contained kanamycin (100 μg/mL). Chemical shifts (δ) are shown in parts per million (ppm), and coupling constants (J) are quoted in Hz.

4.2. Identification of Biotransformation Activity of B. subtilis ATCC 6633 to Curcumin

B. subtilis ATCC 6633 was grown in 50 mL of potato dextrose culture medium (boiled extraction of 200 g/L of peeled potato, 3 g/L of K_2HPO_4, 1.5 g/L of $MgSO_4$, 10 mg/L of Vitamin B1, 20 g/L of glucose) at 180 rpm and 28 °C. After cultivated for 24 h, 1 mg of the curcumin dissolved in 0.1 mL of dimethyl sulfoxide (DMSO) was added into this medium. Subsequently, the culture was extracted by 50 mL of ethyl acetate for three times after 16 h of fermentation. Then, the organic phase was concentrated under vacuum and dissolved in methanol for HPLC analysis in order to assess the biotransformation activity. The identification of biotransformation activity was analyzed by a reverse-phase C18 column (4.6 × 250 mm, 5 μm particles; Welch, Shanghai, China), which was concatenated to an Agilent 1260 HPLC system (ChemStation, B.04.03, Agilent Technologies, Santa Clara, CA, USA) using acetonitrile (solvent B) and 0.5% acetic acid–20 mM ammonium acetate (solvent D) as mobile phases. The gradient program was at 20–40% B for 15 min, 40–55% B for 10 min, 55–95% B for 13 min, 95–20% B for 2 min, and 20% B for 5 min over 45 min at a flow rate of 1 mL/min. The glycosylated products were detected using UV (425 nm) absorbance.

4.3. Expression and Purification of Recombinant BsGT1 and BsGT2

The genomic DNA was extracted from *B. subtilis* ATCC 6633 using a Takara DNAiso Kit (Takara, Dalian, China). Then, the *BsGT1* and *BsGT2* target genes were amplified from the genomic DNA by PCR, and the primer sets were as follows: forward: 5′-CGGGATCCATGAAAAAGTACCAT ATTTCGA-3′, reverse: 5′-CCGCTCGAGTTACTGCGGGACAGCGGATTT-3′ for *BsGT1*, forward: 5′-CGGGATCCA TGAAGACAGTATTGATTTTGA-3′, reverse: 5′-CCGCTCGAGTTATTTGTTTTTTTGGCGAAT-3′ for *BsGT2*. Restriction enzyme recognizing sites were designed as *Bam*H I (GGATCC) of the forward primer and *Xho* I (CTCGAG) of the reverse primer for the two *BsGT*s. The target genes were subcloned into restriction sites of pET-28a (+) to obtain the expression vector pET-28a-*BsGT*, whose N-terminal fusion with His-tag allowed the expressed proteins to be purified by a Ni-NTA affinity column. Then, the recombinant vector was introduced into *E. coli* BL21 (DE3) via heat shock method to form the recombinant *E. coli*.

The recombinant *E. coli* BL21 strains were cultivated in LB medium (10 g/L of peptone, 5 g/L of yeast extract, 10 g/L of NaCl) at 200 rpm and 37 °C until the optical density was tested to 0.7–0.8 at 600 nm. Then, isopropyl-β-D-thiogalact-opyranoside was added to a final concentration of 0.5 mM, and the strains were further cultured at 18 °C for 16–18 h. The recombinant *E. coli* BL21 strains were harvested through centrifugation (8000 rpm, 10 min, 4 °C) and resuspended in 20 mL of lysis buffer (300 mM of NaCl, 50 mM of NaH_2PO_4, pH 8.0). Then, the disrupted cells were sonicated on ice.

After the cell disruption, liquid was centrifuged at 8000 rpm for 10 min at 4 °C, and the supernatant was loaded onto a pre-equilibrated Ni-NTA column at 4 °C and washed by washing buffer containing 10–250 mM of imidazole gradient according to the manufacturer's directions. The two target proteins were both eluted by elution buffer, which contained 50 mM of imidazole. Then, the concentrated fractions contained target proteins to 1 mL using a 15-mL 10-kDa MWCO (Molecular Weight Cut Off) filter (EMD Millipore, San Diego, CA, USA). After desalination, 20% glycerol was added to the purified proteins solutions, and then they were stored at −70 °C or analyzed by SDS-PAGE.

4.4. Preparative-Scale Reactions and Structural Analysis of the Glucosidic Derivatives

The preparative-scale reaction was conducted using 500 μg of two proteins in 20 mL of reaction buffer contained 2.46 mM of UDP-Glc, 50 mM of Tris-HCl pH 8.0, 20 mM of Mn^{2+}, and 30 mg of substrate solution (dissolved in DMSO). The reactions were incubated at 30 °C or 40 °C for 12 h and extracted with 20 mL of ethyl acetate by three times. Then, the organic phase was concentrated and dissolved in 1.5 mL of methanol, and the substrates and glycosylated products were separated through silica gel column chromatography (200–300 mesh, Marine, Qingdao, China), which were eluted with dichloromethane-methanol (40:1 and 9:1, v/v). The structures of glycosylated products were characterized by ^{1}H NMR and ^{13}C NMR.

The structures were identified using ^{1}H NMR and ^{13}C NMR. The NMR spectra were obtained on either a Bruker AV-500 or Bruker AV-600 spectrometer (Bruker, Billerica, MA, USA) with DMSO-*d6* or acetone-*d6* as the solvent and TMS (tetramethylsilane) as the internal standard.

4.5. Enzyme Activity Assay, Optimal Catalyzing Conditions, and Kinetic Parameters of BsGT1 and BsGT2 toward Curcumin

Enzyme activity assay was conducted with 5 μg of two purified proteins in 300 μL of reaction buffer (50 mM of Tris-HCl pH 8.0) containing 1.37 mM of UDP-Glc and 2 μL of substrates (10 mg dissolved, respectively, in 500 μL of DMSO) and maintained at 37 °C for 3 h. The assays were quenched by adding 600 μL of ethyl acetate for extraction; then, 500 μL was drawn and volatilized in a water bath at 55 °C. Subsequently, 200 μL of chromatographic pure methanol was added for HPLC and LC-MS analysis, which was performed on Agilent 1260-6530 HPLC-QTOF-MS (Agilent Technologies, Santa Clara, CA, USA). Then, the Agilent 6530 Q-TOF mass spectrometer (Agilent Technologies, Santa Clara, CA, USA) was equipped with an electrospray ionization (ESI) source to implement the MS analysis. Data acquisition and analysis were conducted on an Agilent Mass Hunter Workstation software version B.07.00 (Agilent Technologies, Santa Clara, CA, USA).

To confirm the optimal catalyzing condition of curcumin, the catalytic activity of *BsGT1* and *BsGT2* at several different temperatures, pH values, and metal ions were tested. The standard condition was conducted with 5 μg of two purified proteins in 300 μL of the reaction system, which contained 1.37 mM of UDP-Glc, 50 mM of Tris-HCl pH 8.0, 20 Mm of Mn^{2+}, and 2 μL of substrate solution (10 mg of substrates dissolved in 500 μL of DMSO, respectively) and maintained at 40 °C for 3 h, and the temperature, pH, or metal ions in the standard condition were replaced by that of the tested condition. For metal ion testing, 20 mM of $MgCl_2$, $CaCl_2$, $MnCl_2$, or $ZnCl_2$ was used. For pH testing, glycine-NaOH buffer (pH 9.0) and Tris buffer (pH 7.0 and 8.0) were used. Then, the reactions were treated by the method described above and analyzed by HPLC. The conversion ratio was calculated by dividing the area of the substrate peaks of the reaction in the HPLC profile by that of the summation of the substrate and product peaks.

The kinetic parameters of *BsGT1* and *BsGT2* toward curcumin were determined. Kinetic parameters (300 μL) toward curcumin in varying concentrations (36 to 360 μM) were conducted with purified *BsGT1* and *BsGT2*, 50 mM of Tris-HCl pH 8.0, 1.37 mM of UDP-Glc, and 2 μL of substrates solution. The reactions were incubated for 2 min, 4 min, 6 min, 8 min, and 10 min at 37 °C, and then terminated by adding 600 μL of ethyl acetate. All the subsequent steps were carried out as described above, and the kinetic parameters were calculated by Michaelis–Menten equation analysis utilizing GraphPad

Prism version 5.01. Besides, the Kcat values were computed utilizing the predicted molecular mass of 44.0 kDa for *BsGT1* and 44.5 kDa for *BsGT2*.

4.6. Solubility Test

To determine the solubility of curcumin and its glucoside, each compound was dissolved in 1 mL of phosphate-buffered saline (PBS) solution at pH 7.4 followed by vortexing for 30 min and centrifuging at 12,000× g for 15 min at room temperature. Then, aliquots were filtered by a 0.45-µm syringe filter, and an equal volume of methanol was added to analyze by HPLC at UV 425 nm. The concentrations of curcumin and its glucoside were measured based on their peak areas utilizing calibration curves determined by the HPLC of authentic samples.

4.7. Phylogenetic Analysis and Sequence Alignment

The phylogenetic tree was constructed with MEGA version 7.0 among 20 selected functionally characterized GTs from different species using the neighbor-joining method. After phylogenetic tree analysis, the predicted amino acid sequences of *BsGT1* (GenBank accession No. MK173044) and *BsGT2* (GenBank accession No. MK173045) were aligned in DNAMAN version 8.0 based on ClustalW multiple alignments. The sequences' GenBank accession numbers and organisms are as shown below: *YjiC* (AAU40842.1) from *Bacillus licheniformis* DSM 13, *OleD* (ABA42119.1) from *Streptomyces antibioticus*, *BcGT1* (AAS41089.1) and *BcGT12* (AAS41578.1) from *Bacillus cereus* ATCC 10987, *Bs-YjiC* (NP_389104.1) from *Bacillus subtilis* 168, *BsGT110* (WP_003220110) from *Bacillus subtilis* ATCC 6633, *MhGT1* (AQX36236.1) from *Mucor hiemalis* CGMCC 3.14114, *LanGT2* (AAD13553.1) from *Streptomyces cyanogenus*, *GtfD* (AAB49298.1) from *Amycolatopsis orientalis*, *SnogD* (AAF01811.1) from *Streptomyces nogalater*, *CalG1* (AAM70336.1) from *Micromonospora echinospora*, *CaUGT2* (BAD29722.1) from *Catharanthus roseus*, *UGT73AE1* (AJT58578.1) from *Carthamus tinctorius*, *CsUGT73A20* (ALO19886.1) from *Camellia sinensis*, *UGT73B6* (AAS55083.1) from *Rhodiola sachalinensis*, *UGT72B1* (OAP00532.1) from *Arabidopsis thaliana*, *XcGT2* (AAM41712.1) from *Xanthomonas campestris* pv. *campestris* ATCC 33913, *BmGT* (WP_010333859.1) from *Bacillus mojavensis*, *Ba-YjiC* (AKL83970.1) from *Bacillus atrophaeus* UCMB-5137, *BcGT2* (AAS41578.1) from *Bacillus cereus* ATCC 10987, and *YdhE* (AKL83209.1) from *Bacillus atrophaeus* UCMB-5137.

5. Conclusions

Studies of microbial GTs have attracted increasing interest and achieved tremendous progress in the enzymatic O-glycosylation of both natural and unnatural compounds, such as ginsenosides [17,20,23,24], antibiotics [25,26], glycopeptides [27,28], flavonoids [18,29–31], and other polyphenols [19,32]. In this study, compared with *YjiC* from *Bacillus licheniformis* DSM 13, *CaUGT2* from *Catharanthus roseus*, and *UGT76G1* from *Stevia rebaudiana* catalyzing curcumin to diglucoside and monoglucoside [33–35], *BsGT1* and *BsGT2* could catalyze curcumin and its two analogues to only their monoglucosides, which indicate that the two GTs are highly selective to the single phenolic hydroxyl group of such compounds. Herein, the two GTs are expected to biosynthesize the monoglucosides of such hydrophobic polyphenol compounds.

Sequence alignment demonstrated that *BsGT1* and *BsGT2* showed obviously high homology and similarity with the PSPG motif, which can replace plant-derived GTs with biosynthetic natural and natural-like high-value glucosides through overcoming the drawbacks of plant-derived GTs, such as low efficiency in the engineering bacteria. It also provides an effective approach by motif evolution mining the efficient microbial UGTs for application in the biosynthesis of plant-derived rare glucosides. Moreover, microbial GTs are generally more promiscuous than plant-derived GTs toward both the aglycon acceptors and the sugar donors [36], which enables the process of diversification of NPs by conjugating a number of sugar donors to a large range of aglycon acceptors to generate an array of structurally different natural and natural-like products for drug development. In addition, *BsGT1* has a closer phylogenetic relationship with *Bs-YjiC*, which is a promiscuous GT from *Bacillus subtilis*

168, indicating that *BsGT1* may largely possess similar substrate flexibility and power regiospecificity as that of *Bs-YjiC*, which can be exploited as another effective biocatalyst for the glycosylation of both natural and unnatural products with diverse scaffolds.

Overall, our study provides insights into the enzymatic synthesis of curcumin and its two analogues monoglucosides, expands the enzymatic approach to obtain natural and natural-like glucosides in drug discovery and development, and also provides a useful method to ameliorate the aqueous solubility of active compounds.

Supplementary Materials: The following are available online at http://www.mdpi.com/2073-4344/9/9/734/s1: Figure S1: HPLC-QTOF-MS analysis of curcumin biotransformed by *B. subtilis* ATCC 6633; Figure S2: Biotransformation of Curcumin **1** (a) and its two analogues **2** (b) and **3** (c) by the purified *BsGT1*; Figure S3: Biotransformation of curcumin **1** (a) and its two analogues **2** (b) and **3** (c) by the purified *BsGT2*; Figure S4: ^{13}C NMR (a) and ^{1}H NMR (b) analysis of curcumin 4′-O-β-D-glucoside **1a**; Figure S5: ^{13}C NMR (a) and ^{1}H NMR (b) analysis of monoglucoside **2a**; Figure S6: ^{13}C NMR (a) and ^{1}H NMR (b) analysis of monoglucoside **3a**; Figure S7: Kinetic parameters of *BsGT1* (a) and *BsGT2* (b) toward curcumin.

Author Contributions: Conceptualization, J.Z. and W.W.; methodology, formal analysis and investigation, Y.C., Y.S. and Y.X.; resources, H.G. and B.Y.; writing—original draft preparation, Y.C., J.Z. and W.W.; writing—review and editing, Y.C., J.Z. and W.W.; project administration and supervision, J.Z. and W.W.; funding acquisition, W.W.

Funding: This research was funded by Jiangsu Planned Projects for Postdo ctoral Research Funds awarded to Wei-Wei Wang and the grant number is 2018K085B.

Acknowledgments: For the kind gift of *B. subtilis* ATCC 6633, we thank Prof. J. P. N. Rosazza of the University of Iowa (USA).

Conflicts of Interest: The authors proclaim no conflict of interest.

References

1. Scartezzini, P.; Speroni, E. Review on some plants of Indian traditional medicine with antioxidant activity. *J. Ethnopharmacol.* **2000**, *71*, 23–43. [CrossRef]
2. Schmandke, H. D-Limonene in citrus fruit with anticarcinogenic action. *Ernährungs Umschau* **2003**, *50*, 264–266.
3. Kant, V.; Gopal, A.; Pathak, N.N.; Kumar, P.; Tandan, S.K.; Kumar, D. Antioxidant and anti-inflammatory potential of curcumin accelerated the cutaneous wound healing in streptozotocin-induced diabetic rats. *Int. Immunopharmacol.* **2014**, *20*, 322–330. [CrossRef] [PubMed]
4. Vallianou, N.G.; Evangelopoulos, A.; Schizas, N.; Kazazis, C. Potential anticancer properties and mechanisms of action of curcumin. *Anticancer Res.* **2015**, *35*, 645–651. [PubMed]
5. Zhang, S.S.; Gong, Z.J.; Li, W.H.; Wang, X.; Ling, T.Y. Antifibrotic effect of curcumin in TGF-beta 1-induced myofibroblasts from human oral mucosa. *Asian. Pac. J. Cancer. Prev.* **2012**, *13*, 289–294. [CrossRef] [PubMed]
6. Hashish, E.A.; Elgaml, S.A. Hepatoprotective and Nephroprotective Effect of Curcumin Against Copper Toxicity in Rats. *Indian. J. Clin. Biochem.* **2016**, *31*, 270–277. [CrossRef] [PubMed]
7. Aggarwal, B.B.; Harikumar, K.B. Potential therapeutic effects of curcumin, the anti-inflammatory agent, against neurodegenerative, cardiovascular, pulmonary, metabolic, autoimmune and neoplastic diseases. *Int. J. Biochem. Cell. Biol.* **2009**, *41*, 40–59. [CrossRef]
8. Lee, W.H.; Loo, C.Y.; Bebawy, M.; Luk, F.; Mason, R.S.; Rohanizadeh, R. Curcumin and its derivatives: Their application in neuropharmacology and neuroscience in the 21st century. *Curr. Neuropharmacol.* **2013**, *11*, 338–378. [CrossRef]
9. Burgos-Moron, E.; Calderon-Montano, J.M.; Salvador, J.; Robles, A.; Lopez-Lazaro, M. The dark side of curcumin. *Int. J. Cancer.* **2010**, *126*, 1771–1775. [CrossRef]
10. Baell, J.B. Feeling Nature's PAINS: Natural Products, Natural Product Drugs, and Pan Assay Interference Compounds (PAINS). *J. Nat. Prod.* **2016**, *79*, 616–628. [CrossRef]
11. Chin, D.; Huebbe, P.; Pallauf, K.; Rimbach, G. Neuroprotective properties of curcumin in Alzheimer's disease–merits and limitations. *Curr. Med. Chem.* **2013**, *20*, 3955–3985. [CrossRef] [PubMed]
12. Nelson, K.M.; Dahlin, J.L.; Bisson, J.; Graham, J.; Pauli, G.F.; Walters, M.A. The Essential Medicinal Chemistry of Curcumin. *J. Med. Chem.* **2017**, *60*, 1620–1637. [CrossRef] [PubMed]
13. Lee, H.S.; Thorson, J.S. Development of a universal glycosyltransferase assay amenable to high-throughput formats. *Anal. Biochem.* **2011**, *418*, 85–88. [CrossRef] [PubMed]

14. Palcic, M.M. Glycosyltransferases as biocatalysts. *Curr. Opin. Chem. Biol.* **2011**, *15*, 226–233. [CrossRef] [PubMed]
15. Thibodeaux, C.J.; Melancon, C.E.; Liu, H.W. Unusual sugar biosynthesis and natural product glycodiversification. *Nature* **2007**, *446*, 1008–1016. [CrossRef] [PubMed]
16. Taniguchi, N.; Honke, K.; Fukuda, M.; Narimatsu, H.; Yamaguchi, Y.; Angata, T. *Handbook of Glycosyltransferases and Related Genes*; Springer: Berlin/Heidelberg, Germany, 2002; pp. 885–903.
17. Dai, L.; Li, J.; Yang, J.; Zhu, Y.; Men, Y.; Zeng, Y.; Cai, Y.; Dong, C.; Dai, Z.; Zhang, X.; et al. Use of a Promiscuous Glycosyltransferase from *Bacillus subtilis* 168 for the Enzymatic Synthesis of Novel Protopanaxatriol-Type Ginsenosides. *J. Agric. Food. Chem.* **2018**, *66*, 943–949. [CrossRef] [PubMed]
18. Pandey, R.P.; Li, T.F.; Kim, E.H.; Yamaguchi, T.; Park, Y.I.; Kim, J.S.; Sohng, J.K. Enzymatic synthesis of novel phloretin glucosides. *Appl. Environ. Microbiol.* **2013**, *79*, 3516–3521. [CrossRef]
19. Feng, J.; Zhang, P.; Cui, Y.; Li, K.; Qiao, X.; Zhang, Y.T.; Li, S.M.; Cox, R.J.; Wu, B.; Ye, M.; et al. Regio and Stereo-specific O-Glycosylation of Phenolic Compounds Catalyzed by a Fungal Glycosyltransferase from *Mucor hiemalis*. *Adv. Synth. Catal.* **2017**, *359*, 995–1006. [CrossRef]
20. Wang, W.W.; Xu, S.H.; Zhao, Y.Z.; Zhang, C.; Zhang, Y.Y.; Yu, B.Y.; Zhang, J. Microbial hydroxylation and glycosylation of pentacyclic triterpenes as inhibitors on tissue factor procoagulant activity. *Bioorg. Med. Chem. Lett.* **2017**, *27*, 1026–1030. [CrossRef]
21. Lim, E.K. Plant glycosyltransferases: Their potential as novel biocatalysts. *Chemistry* **2005**, *11*, 5486–5494. [CrossRef]
22. Ge, H.X.; Chen, L.; Zhang, J.; Kou, J.P.; Yu, B.Y. Inhibitory effect of curcumin analogs on tissue factor procoagulant activity and their preliminary structure–activity relationships. *Med. Chem. Res.* **2013**, *22*, 3242–3246. [CrossRef]
23. Luo, S.L.; Dang, L.Z.; Zhang, K.Q.; Liang, L.M.; Li, G.H. Cloning and heterologous expression of UDP-glycosyltransferase genes from *Bacillus subtilis* and its application in the glycosylation of ginsenoside Rh1. *Lett. Appl. Microbiol.* **2015**, *60*, 72–78. [CrossRef] [PubMed]
24. Wang, D.D.; Jin, Y.; Wang, C.; Kim, Y.J.; Perez, Z.E.J.; Baek, N.I.; Mathiyalagan, R.; Markus, J.; Yang, D.C. Rare ginsenoside Ia synthesized from F1 by cloning and overexpression of the UDP-glycosyltransferase gene from *Bacillus subtilis*: Synthesis, characterization, and in vitro melanogenesis inhibition activity in BL6B16 cells. *J. Ginseng. Res.* **2018**, *42*, 42–49. [CrossRef] [PubMed]
25. Wu, C.Z.; Jang, J.H.; Woo, M.; Ahn, J.S.; Kim, J.S.; Hong, Y.S. Enzymatic glycosylation of nonbenzoquinone geldanamycin analogs via *Bacillus* UDP-glycosyltransferase. *Appl. Environ. Microbiol.* **2012**, *78*, 7680–7686. [CrossRef] [PubMed]
26. Liu, Y.; Qin, W.; Liu, Q.; Zhang, J.; Li, H.; Xu, S.; Ren, P.; Tian, L.; Li, W. Genome-wide identification and characterization of macrolide glycosyltransferases from a marine-derived *Bacillus* strain and their phylogenetic distribution. *Environ. Microbiol.* **2016**, *18*, 4770–4781. [CrossRef] [PubMed]
27. Huo, Q.; Li, H.M.; Lee, J.K.; Li, J.; Ma, T.; Zhang, X.; Dai, Y.; Hong, Y.S.; Wu, C.Z. Biosynthesis of Novel Glucosides Geldanamycin Analogs by Enzymatic Synthesis. *J. Microbiol. Biotechnol.* **2016**, *26*, 56–60. [CrossRef] [PubMed]
28. Solenberg, P.J.; Matsushima, P.; Stack, D.R.; Wilkie, S.C.; Thompson, R.C.; Baltz, R.H. Production of hybrid glycopeptide antibiotics in vitro and in Streptomyces toyocaensis. *Chem. Biol.* **1997**, *4*, 195. [CrossRef]
29. Chiang, C.M.; Wang, T.Y.; Yang, S.Y.; Wu, J.Y.; Chang, T.S. Production of New Isoflavone Glucosides from Glycosylation of 8-Hydroxydaidzein by Glycosyltransferase from *Bacillus subtilis* ATCC 6633. *Catalysts* **2018**, *8*, 387. [CrossRef]
30. Yoon, J.A.; Kim, B.G.; Lee, W.J.; Lim, Y.; Chong, Y.; Ahn, J.H. Production of a novel quercetin glycoside through metabolic engineering of *Escherichia coli*. *Appl. Environ. Microbiol.* **2012**, *78*, 4256–4262. [CrossRef]
31. Gurung, R.B.; Kim, E.H.; Oh, T.J.; Sohng, J.K. Enzymatic synthesis of apigenin glucosides by glucosyltransferase (YjiC) from *Bacillus licheniformis* DSM 13. *Mol. Cells.* **2013**, *36*, 355–361. [CrossRef]
32. Jeon, Y.M. Enzymatic Glycosylation of Phenolic Compounds Using BsGT-3 Based on Molecular Docking Simulation. *J. Korean Soc. Appl. Bi.* **2009**, *52*, 98–101. [CrossRef]
33. Gurung, R.B.; Gong, S.Y.; Dhakal, D.; Le, T.T.; Jung, N.R.; Jung, H.J.; Oh, T.J.; Sohng, J.K. Erratum to: Synthesis of Curcumin Glycosides with Enhanced Anticancer Properties Using One-Pot Multienzyme Glycosylation Technique. *J. Microbiol. Biotechnol.* **2018**, *28*, 347. [CrossRef] [PubMed]

34. Kaminaga, Y.; Sahin, F.P.; Mizukami, H. Molecular cloning and characterization of a glucosyltransferase catalyzing glucosylation of curcumin in cultured *Catharanthus roseus* cells. *FEBS Lett.* **2004**, *567*, 197–202. [CrossRef] [PubMed]
35. Dewitte, G.; Walmagh, M.; Diricks, M.; Lepak, A.; Gutmann, A.; Nidetzky, B.; Desmet, T. Screening of recombinant glycosyltransferases reveals the broad acceptor specificity of stevia UGT-76G1. *J. Biotechnol.* **2016**, *233*, 49–55. [CrossRef] [PubMed]
36. Song, M.C.; Kim, E.; Ban, Y.H.; Yoo, Y.J.; Kim, E.J.; Park, S.R.; Pandey, R.P.; Sohng, J.K.; Yoon, Y.J. Achievements and impacts of glycosylation reactions involved in natural product biosynthesis in prokaryotes. *Appl. Microbiol. Biotechnol.* **2013**, *97*, 5691–5704. [CrossRef] [PubMed]